

# Relativistic effects in electron vortex states

RUBEN VAN BOXEM<sup>1</sup>, JO VERBEECK<sup>1</sup> and BART PARTOENS<sup>1</sup>

<sup>1</sup> *EMAT & CMT, University of Antwerp - Groenenborgerlaan 171, 2020 Antwerp, Belgium*

PACS 03.65.Pm – Relativistic wave equations  
PACS 03.65.Vf – Phases: geometric; dynamic or topological  
PACS 03.65.Sq – Semiclassical theories and applications

**Abstract** – The recent discovery of electron vortices opens up a wide research domain previously unexplored. The present paper explores the relativistic properties of these singular fermion beams, and quantifies deviations from classical wave theory. It is common in electron optics to use the Schrödinger equation neglecting spin. The present paper investigates the role of spin and the total angular momentum  $J_z$  and how it pertains to the vortex states. As an application, we also investigate if it is possible to use holographic reconstruction to create novel total angular momentum eigenstates with a space-dependent spin polarization in a Transmission Electron Microscopy (TEM) setup. It is demonstrated that relativistic effects disappear in the paraxial limit, and spin effects in holographically created electron vortex beams can be safely ruled out.

**Introduction.** – Singular optics is the study of light waves with a phase singularity [1]. For two decades, since the experimental discovery of optical vortices [2], study of singular properties in the scalar theory of light has led to fascinating applications in various areas of physics [3–8]. Much more recently, the concepts and experimental setups from singular optics found their way to electron microscopes [9,10]. Different methods are being investigated for the production of electron vortices [11,12] and possible applications at the nanoscale are surfacing [13]. The first steps into developing a theory of electron vortices have been taken [14–16]. The quantum mechanical description of electron optics coincides for the most part with scalar optics. This is not surprising due to the fact that for stationary states, both the Maxwell and Schrödinger equations take on the exact same form.

Both photon polarization and electron spin determine a spin angular momentum (SAM) vector, which contributes together with the orbital angular momentum (OAM) vector to the total angular momentum (TAM) vector:  $\mathbf{J} = \mathbf{L} + \mathbf{S}$ . In this paper, the cylindrically symmetric case is studied, and the quantities of interest are the projections of the angular momenta on the  $z$ -axis (parallel to beam propagation):  $J_z = L_z + S_z$ . In what follows, cylindrical symmetry is assumed, and all references to “angular momentum” refer to the projected angular momenta on the vertical  $z$ -axis. One can pose the question of the influence of the bosonic nature of the photon versus the fermionic character of the electron. Electrons have half-

integer spin, which translates to half-integer TAM as a proper observable, where photons have integer SAM, and thus integer TAM. The difference in TAM is elucidated by inspecting the Dirac equation, for which  $L_z$  is not a good quantum number, and it is only the TAM  $J_z$  that commutes with the Dirac Hamiltonian. It may therefore come as a surprise that the scalar theory works so well for fast electron waves. Yet experiments show that electron vortex beams behave as their scalar counterparts, and e.g. spin seems to have little to no influence in the entire TEM (Transmission Electron Microscopy) image formation process [17–19], depending on the acceleration voltage used. This is caused by the relatively small magnitude of the spin effects (or conversely, the high electromagnetic fields required to show the effects), and here it is shown that in the paraxial limit one can speak of proper  $L_z$  eigenstates even in Dirac theory.

Once electron spin comes into play, there are two scalar components (at least in the non-relativistic Pauli case) that cooperatively determine the overall quantifiable properties of the beam. These components are independent if there is no external magnetic field. This leads to the possibility of distinct  $J_z$  eigenstates, which possess interesting properties such as a skyrmionic spin distribution [20]. We pose the question whether such  $J_z$  states can be produced in similar ways as the  $L_z$  eigenstates, e.g. using holographic masks [9,10]. In what follows, natural units are used:  $\hbar = c = 1$ . Operator expectation values are denoted  $\langle O \rangle$ . When the state is an eigenstate, its values are

denoted without brackets as  $O$ .

**Phase singularities and electron vortices.** – The simplest description (using a scalar wave theory) of a phase singularity in the paraxial regime in a transverse plane can be written down in terms of the wave function (or in optics, the electric field  $E$ ), with a singular phase factor:

$$\Psi(r, \varphi) = e^{im\varphi} \psi(r). \quad (1)$$

One can readily see that this is an OAM eigenstate:  $\hat{L}_z \Psi = -i\partial_\varphi \Psi = m\Psi$ . The phase increases linearly with  $\varphi$ , resulting in a singular point at  $r = 0$  in the center of the circular phase ramp, where the phase is undefined. Experimental production of these types of wave functions can be accomplished by using computer-generated holograms [10]. These binary masks can be calculated from the interference of a tilted plane wave with the target vortex mode. Using the principles of holographic reconstruction, illuminating the mask with the reference beam generates the target wave as output. In the case of binary masks, one also gets several higher diffraction orders in the far field. This scalar optics technique allows to create any OAM and even superpositions of  $L_z$  are possible. Exactly the same technique was used with fast electron waves creating specific OAM states and superpositions in [21]. To understand why a scalar theory apparently is sufficient for describing particles with spin we will first consider the non-relativistic Pauli equation.

#### OAM Pauli spinors. –

*Mathematical solutions.* The non-relativistic equation of choice to describe electron polarization is the 2-component Pauli equation. It provides a non-relativistic description of spin and its interaction with electromagnetic fields, which describes the processes in an electron microscope sufficiently. The (stationary) Pauli equation (assuming  $\psi \propto \Psi(\mathbf{r})e^{-iEt}$ ) with an electromagnetic field can be written as follows,

$$\left( \frac{1}{2m} \boldsymbol{\sigma} \cdot (\mathbf{p} - e\mathbf{A}) \right)^2 + e\Phi + \mu_B \boldsymbol{\sigma} \cdot \mathbf{B} \Psi = E\Psi, \quad (2)$$

with vector potential  $\mathbf{A} = (\Phi, \mathbf{A})$  representing an external electromagnetic field,  $\mathbf{B} = \nabla \times \mathbf{A}$ ,  $\phi$  the scalar (electrostatic) potential,  $\boldsymbol{\sigma}$  the Pauli vector,  $e$  the electron's charge,  $\mu_B = \frac{e}{2m}$  the Bohr magneton, and  $\Psi = \begin{pmatrix} \psi^1 \\ \psi^2 \end{pmatrix}$  the 2-component Pauli spinor. In cylindrical symmetry expressed in the coordinates  $(\rho, \varphi, z)$ , the general solutions are readily given by

$$\begin{aligned} \Psi_n^+(\rho, \varphi, z) &= e^{ik_z z} \begin{pmatrix} e^{in\varphi} J_n(\kappa\rho) \\ 0 \end{pmatrix}, \\ \Psi_n^-(\rho, \varphi, z) &= e^{ik_z z} \begin{pmatrix} 0 \\ e^{in\varphi} J_n(\kappa\rho) \end{pmatrix}. \end{aligned} \quad (3)$$

These states are eigenstates of the energy  $E$ , the forward momentum  $k_z$ , the transverse momentum  $\kappa$ , the OAM

$L_z = n$ , and the spin  $S_z$  (labeled with the  $\pm$  superscript), and thus also of  $J_z = L_z + S_z$ . The radial functions  $J_n(x)$  are the  $n$ -th order cylindrical Bessel functions of the first kind. In principle, one can combine any  $\Psi_n^+$  with any other  $\Psi_m^-$  and still have a valid solution, although in general it won't be an  $S_z$  or  $L_z$  eigenstate anymore. The case where  $m = n + 1$  is interesting because this combination is also an eigenstate of the TAM  $J_z = n + \frac{1}{2}$ :

$$\Psi_n^{h_\perp=\pm 1}(\rho, \varphi, z) = e^{ik_z z} \begin{pmatrix} e^{in\varphi} J_n(\kappa\rho) \\ \pm e^{i(n+1)\varphi} J_{n+1}(\kappa\rho) \end{pmatrix}. \quad (4)$$

This state has traded  $L_z$  and  $S_z$  for  $J_z$  and the non-relativistic limit of the transverse helicity  $h_\perp = \boldsymbol{\sigma} \cdot \frac{\mathbf{p} \times \mathbf{e}_z}{|\mathbf{p} \times \mathbf{e}_z|}$ . These states are not OAM eigenstates, and the two scalar spin components have a different OAM. This state's  $L_z$  expectation value is equal to its  $J_z$  eigenvalue:

$$\langle L_z \rangle = \frac{1}{2}[n + (n + 1)] = n + \frac{1}{2} = J_z, \quad (5)$$

This should come as no surprise because  $\langle J_z \rangle = \langle L_z \rangle + \langle S_z \rangle$  and  $\langle S_z \rangle$  is equal to 0 for a spin unpolarized beam. Since the two-component Pauli theory poses no helicity constraints, the transverse spin vector orientation can be defined by choosing an appropriate phase angle between the spin up and spin down component. This can result in a net spin polarization in the transverse plane directly resulting from this relative phase.

*Selection on  $L_z$  by a holographic mask.* Fraunhofer diffraction of a scalar function has been studied extensively in the optics literature using the stationary wave equation:

$$\nabla^2 E + k^2 E = 0. \quad (6)$$

This Helmholtz equation can be derived from the quantum mechanical Schrödinger equation when a stationary state is considered, leading to the same Kirchhoff diffraction formalism applying for light and matter waves. In the case of the 2-component Pauli equation, one has to interpret its spin-less limit leading to the Schrödinger equation. This has been considered formally previously in [22], and the Pauli equation is found to reduce to the Schrödinger equation with the proper probability current only if one considers a spin eigenstate without its interactions with a magnetic field. The effective decoupling of both Pauli spinor components in the absence of an electromagnetic field into two non-interfering components, is entirely consistent in this case and can be described by the following relation:

$$\mathcal{P} \left( \begin{pmatrix} \psi^1 \\ \psi^2 \end{pmatrix} \right) = \mathcal{S}(\psi^1) \otimes \mathcal{S}(\psi^2) = \begin{pmatrix} \mathcal{S}(\psi^1) \\ \mathcal{S}(\psi^2) \end{pmatrix}, \quad (7)$$

where  $\mathcal{P}$  signifies the Pauli and  $\mathcal{S}$  the Schrödinger equation. A spin unpolarized beam diffracting on an  $L_z$  binary fork mask can be described by two separate scalar wave optics systems, each selecting on the same OAM. One effectively has two independent and non-interfering wave

functions undergoing Fraunhofer diffraction, leading to an unpolarized vortex state  $\Psi = \frac{1}{\sqrt{2}}(\Psi_n^+ + \Psi_n^-)$  for unpolarized incidence (see (3)).

A general Pauli electron vortex beam can be parametrized with  $\alpha \in \mathbb{R}$  (the radial functions  $f(r)$  and  $g(r)$  are assumed to be normalized to 1):

$$\Psi(r, \varphi) = \begin{pmatrix} \frac{1}{\sqrt{1+\alpha^2}} e^{in\varphi} f(r) \\ \frac{\alpha}{\sqrt{1+\alpha^2}} e^{in'\varphi} g(r) \end{pmatrix}, \quad (8)$$

where  $n$  and  $n'$  are the two spin components' OAM. This normalized state ( $|\Psi|^2 = 1$ ) is an exact solution of the field-free Pauli equation, but not (in general) an eigenstate of any angular momentum.

If the weight of both components is equal ( $\alpha = 1$ ), one has

$$\langle L_z \rangle = \frac{1}{2}(n + n'), \quad (9)$$

which leads to an  $L_z = n$  eigenstate if  $n = n'$ , and

$$\langle J_z \rangle = \frac{1}{2}[(n + 1/2) + (n' - 1/2)] = \frac{1}{2}(n + n'), \quad (10)$$

which leads to  $\langle J_z \rangle = n$  if  $n = n'$ . So in the case of identical vortices in both spin components, we have  $L_z = \langle J_z \rangle = n$ . In terms of measurable effects, the system behaves as two independent and identically propagating scalar systems in an  $L_z$  eigenstate.

If the weight of both components is not equal, one has for the angular momenta expectation values:

$$\langle L_z \rangle = \frac{n}{1+\alpha^2} + \frac{\alpha^2 n'}{1+\alpha^2} = \frac{n + \alpha^2 n'}{1 + \alpha^2}, \quad (11a)$$

$$\langle S_z \rangle = \frac{\frac{1}{2}}{1+\alpha^2} + \frac{-\frac{1}{2}}{1+\alpha^2} = \frac{1}{2} \frac{1 - \alpha^2}{1 + \alpha^2}, \quad (11b)$$

$$\langle J_z \rangle = \langle L_z + S_z \rangle = \frac{n + \alpha^2 n'}{1 + \alpha^2} + \frac{1}{2} \frac{1 - \alpha^2}{1 + \alpha^2}. \quad (11c)$$

In the special case  $n' = n + 1$ , spinor (8) is an eigenstate of  $J_z$  with eigenvalue  $n + \frac{1}{2}$ , and this is unaffected by the value of  $\alpha$ . The above shows that even though only  $J_z$  is a proper quantum number, for the special case of unpolarized electrons, the  $J_z$  eigenstate also has  $\langle L_z \rangle = J_z$ .

Fig. 1 shows the scalar far field image of an illuminated fork mask, showing clearly the 0th and first order vortices ( $\pm 1$  and  $\pm 2$ ). The third far field image shows the density of a spinor  $J_z$  eigenstate (4), which is the sum of the other two images. It contains two superimposed and independent scalar vortices of different order.

*Selection on  $J_z$  by a holographic mask.* In order to create a  $J_z$  eigenstate such as those in (4), one needs a superposition of different OAM for each spin component. For photons, subwavelength gratings can be used to produce such states [23]. This is difficult for electrons in an electron microscope, as the wavelength of an accelerated

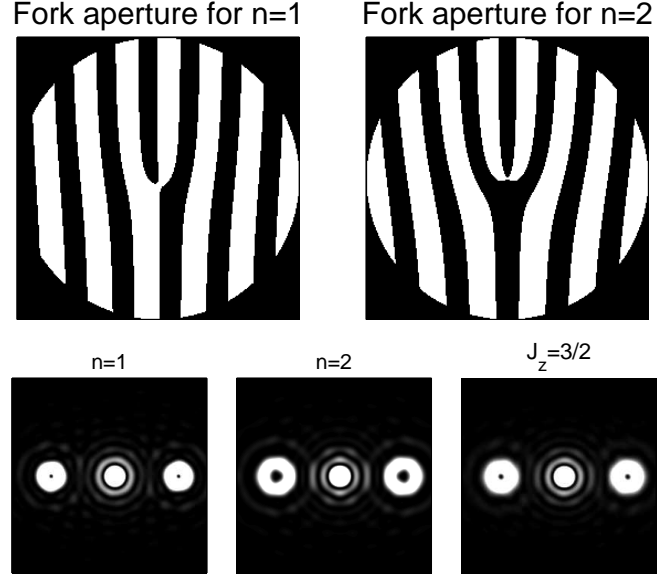


Fig. 1: The farfield of a scalar  $n = 1$ ,  $n = 2$ , and a spinor  $J_z = \frac{3}{2}$  (equation (4)) with the radial distribution caused by a circular aperture with a fork pattern. The doughnut shapes are phase vortices, with a phase ramp of 0 to  $n2\pi$ , and a central zero-density phase singularity. Intensity is saturated which allows direct comparison with fig. 2.

electron is typically of the order of pm. Creating half-integer holographic masks does not have the desired effect. As previously shown by Berry [24], this leads to non-integral OAM which is nothing but the sum of integral OAM contributions, which show in the wave pattern as the interference of the different OAM modes. A holographic mask designed for half integer  $L_z$  will diffract both spin components in exactly the same way, leading to no space-variant polarization as described by Wang et al. [20] for the target states. The relative phase between the two spin components is important for the interference though, as shown in fig. 2 and explained below.

To demonstrate this, we calculated a binary holographic mask from the interference pattern of an unpolarized (in  $z$ -direction) incoming plane wave, and a state of the form (4). Fig. 2 shows several possible masks for  $m = n + 1$  and different relative phases (=transverse spin orientation) between the two spin components of the incoming tilted wave. The reference tilted plane wave used is:

$$\Psi_{\text{Ref}} = e^{ik_z z + ik_x x} \begin{pmatrix} 1 \\ C \end{pmatrix}, \quad (12)$$

where  $C$  is equal to 1,  $-i$ , and  $\frac{1}{2}(1-i)$  for the three figures in fig. 2. As one can clearly see in fig. 2, the relative phase factor between the two spin states (which determines the direction of the transverse spin vector) used to calculate the holographic mask, also determines the orientation of the additional dislocation line and the direction in which the extra integral order vortices split off from the most intense vortex. Once the mask is calculated, it does not

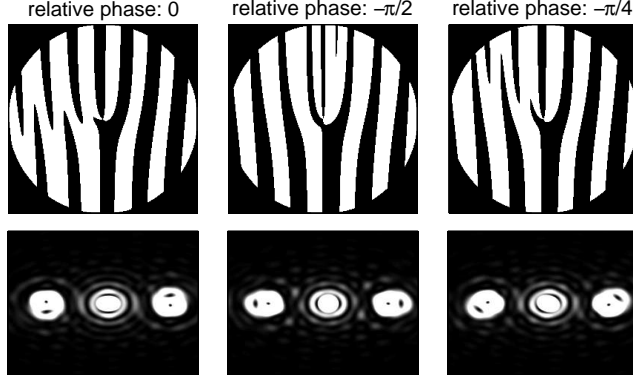


Fig. 2: Above: Holographic binary masks calculated by interfering  $J_z$  eigenstates with different relative phases for the incoming tilted spin states (12). One can see that the relative phase influences the orientation of an additional dislocation line within the mask. Below: Far field images obtained by illuminating the holographic masks with the tilted reference wave. The intensity is saturated to bring forward the structure of the first order vortices. Scalar diffraction gives the same result, and it is not equal to the third image in fig. 1, which shows the wanted  $J_z$  eigenstate.

matter what the phase factor of the illuminating reference wave is; as shown above both components scatter independently, and the incoming beam's spin is of no influence to the resulting interference pattern. Due to considerations expressed in the previous section, this hybrid OAM mask does not lead to the  $J_z$  vortex eigenstates. The resulting wave is not of the desired form nor character, instead breaking down to a combination of integer order vortices. This shows the  $J_z$  eigenstates can only be obtained when we can influence both spin components independently (e.g. as with an electromagnetic field). Fourier reconstruction does give the expected result for spinors.

We will now investigate under what conditions the intrinsic relativistic spin coupling (detailed in the next section) might be exploited in the kinematical regime of a TEM.

### OAM Dirac spinors. –

*Mathematical solutions.* In order to further understand the role of spin and thus the TAM of electron vortex states, the solutions of the cylindrical Dirac equation are considered. The underlying foundation of the question whether  $L_z$  or  $J_z$  is the most important variable, can be answered quantitatively by inspecting the fully relativistically correct cylindrical solutions to the free Dirac equation ( $\gamma^\mu$  are the Dirac matrices,  $\Psi$  is a 4-component Dirac spinor):

$$(i\gamma^\mu \partial_\mu - m) \Psi = 0. \quad (13)$$

Equation (13) admits cylindrically symmetric solutions of the form:

$$\Psi_{n,s}(r, \varphi, z) = e^{i(k_z z - Et)} \times \begin{pmatrix} e^{in\varphi} J_n(k_\perp r) \\ s e^{i(n+1)\varphi} J_{n+1}(k_\perp r) \\ \frac{k_z - isk_\perp}{E+m} e^{in\varphi} J_n(k_\perp r) \\ -s \frac{k_z - isk_\perp}{E+m} e^{i(n+1)\varphi} J_{n+1}(k_\perp r) \end{pmatrix}. \quad (14)$$

These are eigenstates of  $E$ ,  $k_z$ ,  $J_z$ ,  $p_\perp$ , and the transverse helicity defined by  $h_\perp = \gamma^5 \gamma^3 \frac{\Sigma \cdot p_\perp}{|p_\perp|}$ , which takes the values  $\pm 1$ . Taking a similar linear combination as the one that relates the Pauli spinors in equations (3) and (4), one can construct from (14) only an approximate  $L_z$  eigenstate:

$$\Psi_n^{(+)} = \frac{1}{2} (\Psi_{n,s=+1} + \Psi_{n,s=-1}) \propto \begin{pmatrix} e^{in\varphi} J_n(k_\perp r) \\ 0 \\ \frac{k_z}{E+m} e^{in\varphi} J_n(k_\perp r) \\ \frac{ik_\perp}{E+m} e^{i(n+1)\varphi} J_{n+1}(k_\perp r) \end{pmatrix} \quad (15a)$$

$$\Psi_{n-1}^{(-)} = \frac{1}{2} (\Psi_{n-1,s=+1} - \Psi_{n-1,s=-1}) \propto \begin{pmatrix} 0 \\ e^{in\varphi} J_n(k_\perp r) \\ \frac{-ik_\perp}{E+m} e^{i(n-1)\varphi} J_{n-1}(k_\perp r) \\ \frac{-k_z}{E+m} e^{in\varphi} J_n(k_\perp r) \end{pmatrix}. \quad (15b)$$

The solutions in equation (15) bear the closest resemblance to the Pauli spinors discussed above (see (3)). These solutions are still  $J_z$  eigenstates with eigenvalue  $n \pm 1/2$ , and become  $L_z = n$  and  $\Sigma_z$  eigenstates only in the paraxial approximation:  $k_\perp \ll E + m$ . Note that both of these solutions carry a different unapproximated eigenvalue of  $J_z$ , although their approximate  $L_z$  eigenvalue is equal. It is as though the paraxial limit removes the coupling of the electronic wave function to its spin in this field-free case. Bliokh et al. [25] have previously presented an alternative form of (15), but the form here better captures the kinematical quantities that are relevant in a practical TEM experiment. The quantitative analysis of the relativistic spin coupling these solutions contain is presented below.

*Relativistic properties of electron vortex beams.* As previously illuminated by Bliokh et al. [25], there are two special states which, in principle, permit us to directly observe a relativistic effect. There, it is shown that for the states  $\Psi_{-1}^{(+)}$  and  $\Psi_1^{(-)}$  (see (15)), there is a significant central contribution to the density  $\rho$ . Below is shown however that this effect is extremely small for typical TEM parameters. The zeroth order Bessel functions are the only ones that are nonzero at the origin (i.e. the center of the beam). This gives the states  $\Psi_{-1}^{(+)}$  and  $\Psi_1^{(-)}$  (see equation (15)) a

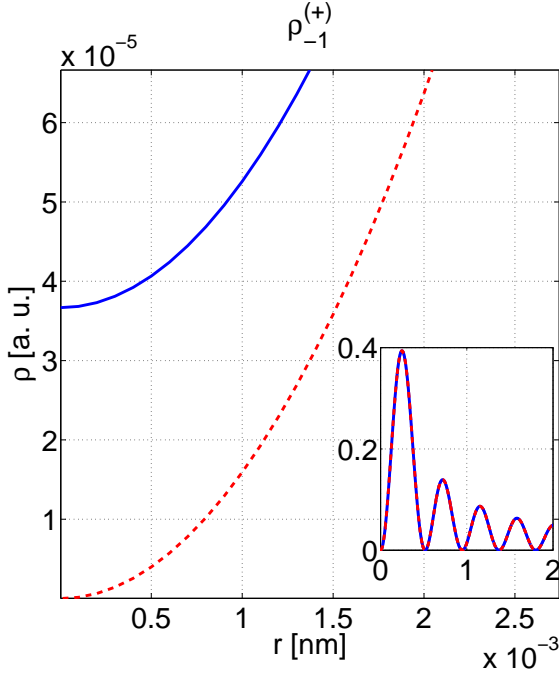


Fig. 3: Central density distribution (16) using the parameters mentioned in the text. The blue (solid) line is given by (16) and the red (dashed) line is only the first term of that equation.

nonzero central density:

$$\rho_{-1}^{(+)}(r) = \rho_1^{(-)}(r) = \left(1 + \frac{k_z^2}{(E+m)^2}\right) J_1^2(k_\perp r) + \frac{k_\perp^2}{(E+m)^2} J_0(k_\perp r). \quad (16)$$

The third term results in a non-zero density at  $r = 0$ , proportional to  $\frac{k_\perp^2}{(E+m)^2}$ . Approximating the radius of the vortex by only looking at the maximum of  $J_1^2$ , one can estimate  $k_\perp$  (up to  $\mathcal{O}((k_\perp r)^4)$ ) for a single- $k_\perp$  state (see Appendix):

$$k_\perp \text{ (in keV)} \approx \frac{0.37 \dots}{R \text{ (in nm)}}. \quad (17)$$

In state of the art TEM experiments, one can achieve a focused electron vortex [10] of  $R \approx 0.5$  Å, and one has  $k_\perp \approx 7.4$  keV. For a 200 keV beam, this results in a central contribution to the density of about  $3.7 \times 10^{-5}$ . This figure needs to be compared with the unity sized contribution of the other terms in (16). Fig. 3 shows a comparison of the first term of (16) with the full expression for the aforementioned values. It should be compared with fig. 2 in [25]. The relativistic effect for these states in this parameter regime are much smaller than the differences shown in that article. By increasing the focus and thus by further shrinking the vortex, one can in principle increase the magnitude of the effect, because  $k_\perp$  increases with decreasing vortex size according to (17). Though as one

increases  $k_\perp$ , the relevant area of the central density will shrink as well. One can easily estimate the radius inside which the zeroth order contribution is larger than the first order in (16) (see Appendix):

$$r_C \approx \frac{0.24 \dots}{\left(k_z^2 + m(m + \sqrt{k_z^2 + m^2})\right)^{1/4}} \sqrt{R} + \dots, \quad (18)$$

where  $R$  is in nm and the kinematic quantities in keV (natural units). For our values of the parameters  $k_\perp$  and  $k_z$ , one has  $r_C \approx 4$  pm, which is of the order of the electron wavelength. The area inside the critical radius is thus of the order of  $50 \text{ pm}^2$ , in which the intensity is equal to approximately  $10^{-5}$  the intensity at the vortex maximum. For a spin-unpolarized beam the oppositely polarized vortex state (see (15)) is also present, which adds another unwanted unity sized background contribution which has to be discriminated upon measurement. The extremely small size of these effects allows us to say with certainty that pure relativistic effect of free-space electron vortices is unobservable for the conditions prevalent in an electron microscope. The smallness of these effects will translate into the fact that the Pauli description suffices, that is to say, (7) is valid, and effectively  $L_z$  can be maintained as a good quantum number even though this is not the case in the Dirac description. The extreme small size of the spin coupling effects in electron vortices lead us to conclude that single-electron diffraction through a holographic mask cannot produce  $J_z$  vortex eigenstates. The Pauli equation supplies enough information for the TEM system and it results in per-spin Fraunhofer diffraction, leading to the coherent sum of the two spin states being present in the resulting diffraction pattern.

**Conclusions.** — This paper has investigated the properties of electron vortex states as they appear in electron microscopes. The question of the right quantum numbers to qualify electron vortex states in a field-free region of space is answered. It is apparent that  $L_z$  is the right quantum number to label free electron vortex states, and neglecting spin in the description of their formation as long as no magnetic effects occur. This follows from the decoupling of the non-relativistic Pauli equation in the absence of an electromagnetic field. In an attempt to quantify the field-free relativistic effects as previously illuminated by Bliokh et al. [25], an alternative form of the Dirac spinors representing approximate  $L_z$  electron vortex eigenstates is presented and their connection to the transverse helicity eigenstates of the Dirac equation is shown. These were used to calculate the size of the contribution of the relativistic description to the central density present in specific states. It was found that for realistic conditions in modern electron microscopes, the field-free relativistic effects are very difficult, if not impossible, to observe: the relative intensity of this central density compared to the maximum of the full wave lies around  $10^{-5}$ , and the size of the area in which the effect dominates is of the order of the electron



wavelength. The current experimental apparatus does not lead to sufficiently large relativistic spin effects, so these cannot be measured.

The usage of a holographic mask to produce  $J_z$  eigenstates was investigated. A holographic fork aperture works spatially, whereas spin is an additional internal degree of freedom not directly related to the spatial diffraction phenomenon. The introduction of an electromagnetic field will couple the two components, and we expect the  $J_z$  eigenstates presented here to become important. One can thus not fabricate a  $J_z$  holographic mask without some form of magnetism, which could in itself lead to transverse spin-splitting as in [26], although it is not clear how the transverse Stern-Gerlach effect calculated there will couple to vortex formation by a holographic mask. A combined magnetized and forked pattern seems like the most achievable solution, once the necessary magnetization conditions can be experimentally achieved. Without magnetization or ultra-relativistic effects, one cannot influence the spin degree of freedom by simple diffraction. In principle, one can repeat the calculations in this paper for neutrons, where perhaps the different interactions and parameters can cause the effects described above to become observable. Neutron vortex states have not been presented as far as the authors are aware, but might bring the rich properties of phase singular beams to neutron optics.

\*\*\*

This research was supported by an FWO PhD fellowship grant (Aspirant Fonds Wetenschappelijk Onderzoek - Vlaanderen). The authors acknowledge financial support from the European Union under the Seventh Framework Program under a contract for an Integrated Infrastructure Initiative. Reference No. 312483-ESTEEM2. J. Verbeeck acknowledges funding from the European Research Council under the 7th Framework Program (FP7), ERC grant N246791 - COUNTATOMS and ERC Starting Grant 278510 VORTEX.

## Appendix. –

*Relation between the radial size of a Bessel beam in nm and  $k_\perp$  in keV.* In what follows no units are specified, because it is assumed  $k_\perp$  has the inverse unit of  $r$ , resulting in a dimensionless argument to the Bessel function. An extremum of the first order Bessel function of the first kind is determined by the following equation:

$$\partial_r J_1(k_\perp r) = 0, \quad (19)$$

which can be rewritten using the Bessel function's recursion relations to read:

$$J_0(k_\perp r) - J_2(k_\perp r) = 0. \quad (20)$$

The next step is expanding the Bessel functions up to order  $(k_\perp r)^4$  around  $k_\perp r = 0$  (which turns out to be a

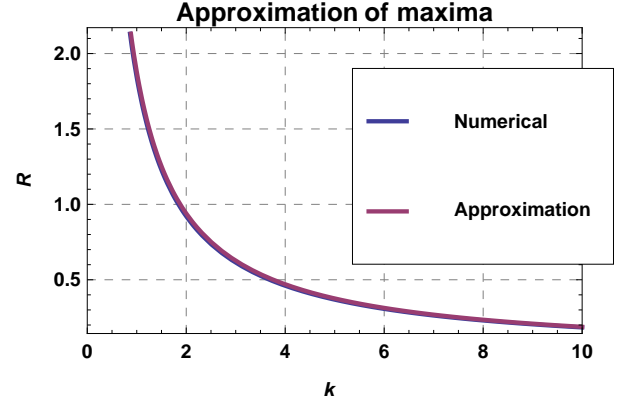


Fig. 4: Approximation of the radius of the vortex in function of  $k_\perp$  for a Bessel beam of order 1. The curves are almost exactly superposed

valid approximation for  $k_\perp > 1$ ). This leads to following even fourth degree equation:

$$1 - \frac{(k_\perp r)^2}{4} + \frac{(k_\perp r)^4}{64} = \frac{(k_\perp r)^2}{8} - \frac{(k_\perp r)^4}{96}. \quad (21)$$

Solving this for  $t = \frac{(k_\perp r)^2}{4}$ , gives the relevant root:

$$\frac{k_\perp r}{2} = \sqrt{0.8835} \Leftrightarrow r = \frac{1.8799}{k_\perp}. \quad (22)$$

The result is shown in figure 4. The maximum relative error in the domain  $k_\perp \in [1, 10]$  of this approximation is under the 0.4%.

The final step is the conversion to natural units ( $\hbar = c = \hbar c = 1$ ), where

$$1 \text{ nm}^{-1} = 197.327 \text{ eV}, \quad (23)$$

and thus for a given radius  $R$  in nm, the transverse momentum of a matching Bessel mode in keV is:

$$k_\perp \approx \frac{0.37 \dots}{R}. \quad (24)$$

*Vortex core size.* By equating the two terms in (16) and expanding the Bessel functions up to  $\mathcal{O}((k_\perp r)^4)$ , one has:

$$\frac{k_\perp^2}{(E+m)^2 + k_z^2} J_0^2(k_\perp r_C) = J_1^2(k_\perp r_C) \\ \alpha \left( 1 - \frac{k_\perp^2 r_C^2}{2} + \frac{3k_\perp^4 r_C^4}{32} + \dots \right) = \frac{k_\perp^2 r_C^2}{4} - \frac{k_\perp^4 r_C^4}{16} + \dots, \quad (25)$$

where  $\alpha = \frac{k_\perp^2}{(E+m)^2 + k_z^2}$ . One has to take note that if  $r_C$  is expressed in nm, one has to introduce a conversion factor from natural units between the  $k_\perp$  in  $\alpha$  and the  $k_\perp$  in (25). The smallest positive root gives an expression for small  $k_\perp$ :

$$\frac{0.33 \dots}{(k_z^2 + m(m + \sqrt{k_z^2 + m^2}))^{1/4} \sqrt{k_\perp}} + \mathcal{O}(\sqrt{k_\perp}). \quad (26)$$

## REFERENCES

- [1] NYE J. F. and BERRY M. V., *Proceedings of the Royal Society of London. A. Mathematical and Physical Sciences*, **336** (1974) 165.  
<http://rspa.royalsocietypublishing.org/content/336/1605/165>
- [2] HECKENBERG N. R., MCDUFF R., SMITH C. P. and WHITE A. G., *Opt. Lett.*, **17** (1992) 221.  
<http://ol.osa.org/abstract.cfm?URI=ol-17-3-221>
- [3] O'NEIL A. T., MACVICAR I., ALLEN L. and PADGETT M. J., *Phys. Rev. Lett.*, **88** (2002) 053601.  
<http://link.aps.org/doi/10.1103/PhysRevLett.88.053601>
- [4] PADGETT M. and BOWMAN R., *Nat. Photon.*, **5** (2011) 343.  
<http://www.nature.com/doi/10.1038/nphoton.2011.81>
- [5] HE H., FRIESE M. E. J., HECKENBERG N. R. and RUBINSZTEIN-DUNLOP H., *Phys. Rev. Lett.*, **75** (1995) 826.  
<http://link.aps.org/doi/10.1103/PhysRevLett.75.826>
- [6] THIDÉ B., THEN H., SJÖHOLM J., PALMER K., BERGMAN J., CAROZZI T. D., ISTOMIN Y. N., IBRAGIMOV N. H. and KHAMITOVA R., *Phys. Rev. Lett.*, **99** (2007) 087701.  
<http://link.aps.org/doi/10.1103/PhysRevLett.99.087701>
- [7] BERKHOUT G. C. G. and BEIJERSBERGEN M. W., *Journal of Optics A: Pure and Applied Optics*, **11** (2009) 094021.  
<http://stacks.iop.org/1464-4258/11/i=9/a=094021>
- [8] GROVER A. SWARTZLANDER J., FORD E. L., ABDUL-MALIK R. S., CLOSE L. M., PETERS M. A., PALACIOS D. M. and WILSON D. W., *Opt. Express*, **16** (2008) 10200.  
<http://www.opticsexpress.org/abstract.cfm?URI=oe-16-14-10200>
- [9] UCHIDA M. and TONOMURA A., *Nature*, **464** (2010) 737.  
<http://www.nature.com/nature/journal/v464/n7289/full/nature08904.html>
- [10] VERBEECK J., TIAN H. and SCHATTSCHEIDER P., *Nature*, **467** (2010) 301.  
<http://www.nature.com/nature/journal/v467/n7313/abs/nature09366.html>
- [11] VERBEECK J., TIAN H. and BÉCHÉ A., *Ultramicroscopy*, **113** (2012) 83.  
<http://www.sciencedirect.com/science/article/pii/S0304399111002531>
- [12] SCHATTSCHEIDER P., STÖGER-POLLACH M., LÖFFLER S., STEIGER-THIRSFELD A., HELL J. and VERBEECK J., *Ultramicroscopy*, **115** (2012) 21.  
<http://www.sciencedirect.com/science/article/pii/S0304399112000113>
- [13] VERBEECK J., TIAN H. and VAN TENDELOO G., *Advanced Materials*, **25** (2013) 1114.  
<http://dx.doi.org/10.1002/adma.201204206>
- [14] SCHATTSCHEIDER P. and VERBEECK J., *Ultramicroscopy*, **111** (2011) 1461.  
<http://www.sciencedirect.com/science/article/pii/S0304399111001811>
- [15] BLOKH K. Y., BLOKH Y. P., SAVEL'EV S. and NORI F., *Phys. Rev. Lett.*, **99** (2007) 190404.  
<http://link.aps.org/doi/10.1103/PhysRevLett.99.190404>
- [16] BLOKH K. Y., SCHATTSCHEIDER P., VERBEECK J. and NORI F., *Phys. Rev. X*, **2** (2012) 041011.  
<http://link.aps.org/doi/10.1103/PhysRevX.2.041011>
- [17] ROTHER A. and SCHEERSCHMIDT K., *Ultramicroscopy*, **109** (2009) 154.  
<http://www.sciencedirect.com/science/article/pii/S0304399108002295>
- [18] FERWERDA H., HOENDERS B. and SLUMP C., *Optica Acta: International Journal of Optics*, **33** (1986) 159.  
<http://www.tandfonline.com/doi/abs/10.1080/713821925>
- [19] JAGANNATHAN R., *Phys. Rev. A*, **42** (1990) 6674.  
<http://link.aps.org/doi/10.1103/PhysRevA.42.6674>
- [20] WANG Y. and LI C.-F., *EPL*, **95** (2011) 44001.  
<http://iopscience.iop.org/0295-5075/95/4/44001>
- [21] GUZZINATI G., SCHATTSCHEIDER P., BLOKH K., NORI F. and VERBEECK J., *ArXiv e-prints*, (2012) .  
<http://arxiv.org/abs/1209.3413>
- [22] GÜRTLER R. and HESTENES D., *Journal of Mathematical Physics*, **16** (1975) 573.  
<http://link.aip.org/link/?JMP/16/573/1>
- [23] GORODETSKI Y., BIENER G., NIV A., KLEINER V. and HASMAN E., *Opt. Lett.*, **30** (2005) 2245.  
<http://ol.osa.org/abstract.cfm?URI=ol-30-17-2245>
- [24] BERRY M. V., *Journal of Optics A: Pure and Applied Optics*, **6** (2004) 259.  
<http://stacks.iop.org/1464-4258/6/i=2/a=018>
- [25] BLOKH K. Y., DENNIS M. R. and NORI F., *Phys. Rev. Lett.*, **107** (2011) 174802.  
<http://link.aps.org/doi/10.1103/PhysRevLett.107.174802>
- [26] MCGREGOR S., BACH R. and BATELAAN H., *New Journal of Physics*, **13** (2011) 065018.  
<http://stacks.iop.org/1367-2630/13/i=6/a=065018>